

Article

Polydopamine-Coated Polyurethane Foam as a Structured Support for the Development of an Easily Reusable Heterogeneous Photocatalyst Based on Eosin Y

Han Peng ¹, Thierry Romero ², Philippe Bertani ³ and Vincent Ritleng ^{1,*} 

¹ École Européenne de Chimie, Polymères et Matériaux, Université de Strasbourg, CNRS, LIMA, UMR 7042, 25 Rue Becquerel, 67087 Strasbourg, France

² École Européenne de Chimie, Polymères et Matériaux, Université de Strasbourg, CNRS, ICPEES, UMR 7515, 25 Rue Becquerel, 67087 Strasbourg, France

³ Institut de Chimie de Strasbourg, Université de Strasbourg, CNRS, UMR 7177, 4 Rue Blaise Pascal, 67081 Strasbourg, France

* Correspondence: vritleng@unistra.fr

Abstract: An easy-to-handle eosin Y-based heterogeneous photocatalyst was prepared by post-functionalization of a polydopamine-coated open cell polyurethane foam (PDA@PUF) via the silanization of the adhesive layer with 3-(triethoxysilyl)propan-1-amine (APTES) and the subsequent EDC-mediated coupling of the resulting amino-functionalized foam with eosin Y. The obtained macroscopic material, EY-APTES@PDA@PUF, showed good efficiency and excellent reusability, in an easy-to-carry “dip-and-play” mode for at least six runs as photocatalyst for the aerobic oxidation of 2-methyl-5-nitroisoquinolin-2-ium iodide to the corresponding isoquinolone. Subsequent investigation of the catalytic efficiency of EY-APTES@PDA@PUF for the oxidation of sulfides to sulfoxides, however, evidenced non-negligible eosin Y leaching, leading to a progressive deactivation of the catalytic foam in this case. Two alternative synthetic protocols for the preparation of the macroscopic photocatalyst were next explored to avoid eosin Y leaching. In both cases however, cycling tests also highlighted a progressive deactivation of the catalytic foams in sulfide-to-sulfoxide oxidation reactions.

Keywords: visible-light photocatalysis; polyurethane open cell foam; polydopamine; eosin Y; oxidation reactions



Citation: Peng, H.; Romero, T.; Bertani, P.; Ritleng, V.

Polydopamine-Coated Polyurethane Foam as a Structured Support for the Development of an Easily Reusable Heterogeneous Photocatalyst Based on Eosin Y. *Catalysts* **2023**, *13*, 589.

<https://doi.org/10.3390/catal13030589>

Academic Editors: Victorio Cadierno and Raffaella Mancuso

Received: 23 February 2023

Revised: 11 March 2023

Accepted: 14 March 2023

Published: 15 March 2023



Copyright: © 2023 by the authors. Licensee MDPI, Basel, Switzerland. This article is an open access article distributed under the terms and conditions of the Creative Commons Attribution (CC BY) license (<https://creativecommons.org/licenses/by/4.0/>).

1. Introduction

Organic photoredox catalysts represent attractive alternatives in visible-light photocatalysis in comparison to expensive and potentially toxic noble metal-based photocatalysts such as [Ru(bpy)₃]Cl₂ or [Ir(dF(CF₃)ppy)₂(bpy)](PF₆). Organic dyes are indeed typically less toxic, easier to handle, and available at lower cost, as they can be readily synthesized from natural feedstock. In addition, they often exhibit superior solubility in organic solvents [1]. The growing interest in their development is also driven by the fact that they often compare to or even outperform transition metal-based photocatalysts [2,3]. Furthermore, due to their inherent potent reactivity, they are much more than simple alternatives to transition metal-based photocatalysts and can enable unique reactivities [4,5].

Among the variety of organic photoredox catalysts [4], eosin Y is by far one of the most studied organic dyes for its photocatalytic properties in organic synthesis [1,6]. In particular, eosin Y has demonstrated high catalytic efficiency in various valuable synthetic transformations, including reductions of nitroarenes [7], oxidations of sulfides and phenylboronic acids [8], oxidative phosphorylations and thiolations of amines [9,10], C–H arylations [11], aldehydic C–H functionalizations by hydrogen atom transfer [5], ketone

trifluoromethylations [12,13], polymerization reactions [14–16], as well as cooperative asymmetric organophotoredox catalysis [17–19]. Despite this impressive versatility, important limitations remain, which hamper the development of large-scale processes.

According to the Beer–Lambert law, photochemical reactions carried out in conventional batch reactors are indeed exposed to a non-uniform distribution of radiation due to the photon transport attenuation effect. Consequently, the reaction medium near the middle or the wall of the reactor will be exposed to different intensities of irradiation, thus causing various reaction rates [6,20]. While this phenomenon can be easily overcome in small reaction flasks by strong stirring, when it comes to large photochemical reactors, this non-uniform irradiation may give rise to (i) the over-irradiation of external zones, generating the formation of undesired byproducts, (ii) dramatically reduced reaction rates [21]. Possible solutions to this issue consist of conducting the catalysis under heterogeneous conditions with the photocatalyst anchored to a solid support, as the light diffusion into the solution will then not be hampered by the high molar extinction coefficient of the dissolved photocatalyst, and/or in flow [6,20]. Additionally, with this method, the workup procedures will be simplified, and the photocatalyst can potentially be easily reused several times. This strategy has already been largely applied to eosin Y with solid supports as varied as silica particles [16], graphene oxide [22], metal-organic frameworks [23,24], polymeric supports [8,25–27], glass wool [28], cotton threads [29], sulfur-doped graphitic carbon nitride [30], or magnetic nanoparticles [31,32]. To the best of our knowledge, eosin Y has however never been supported on a macroscopic structured support such as an open cell foam, which should allow its use and reuse in a “dip-and-play” mode, that means simply immersing it into the liquid reaction medium at the beginning of the process and removing it at the end, therefore avoiding long filtration and centrifugation procedures as are often encountered with powdered heterogeneous catalysts.

Open cell foams provide large surface-to-volume ratios, efficient mass transfers, and small pressure drop. Their open structure along with their macroscopic shape allow an intimate mixing of the reagents, as well as an easy accessibility of the reactants to the active sites, while avoiding a tedious separation of the products from the catalyst [33]. These properties are advantageous in continuous processes. Of metallic or ceramic constitution, these macroscopic structures are perfect candidates for immobilizing catalytically active metallic nanoparticles [34–36]. Their preparation however comprises multiple steps, including high-temperature steps for the production of the macroscopic foams, as well as energy intensive processes for the grafting and activation of the catalytic phase onto the surface [35]. In addition, these metallic or ceramic foams display many disadvantages such as: (i) rigid structures that render them fragile, (ii) the occurrence of randomly distributed closed cells that may affect the reproducibility of the reactions, and (iii) the necessity to carry on numerous chemical treatments in highly corrosive media to recover the metal catalyst before disposal [37].

Due to their commercial availability, affordable prices, interesting mechanical properties, and easiness of engineering [38], polyurethane open cell foams (PUF) presented an interesting possible alternative to ceramic and metallic foams, provided that one could find a chemical or physical mean to deposit the active phase without altering the mechanical and transport properties as PUF are devoid of microporosities. Inspired by a biomimetic approach [39], our group successfully coated PUFs with a thin adhesive layer of polydopamine (PDA) by a simple dip-coating procedure in a buffered (pH 8.5) solution of dopamine in water [40], and applied the resulting flexible PDA@PUF structured support in various dye removal [41–43] or catalytic [44–47] processes after functionalization with metal [42,45,47] or metal oxide [41,46] nanoparticles, molecular catalysts [44], or hydrides [42,43]. The strong adhesive properties of the PDA layer, resulting from a vast array of interactions going from Van de Waals forces to covalent or coordination bonds [48], ensured both a robust coating of PUFs with PDA and a robust anchoring of the active agents on the PDA layer. This property together with the “dip-and-play” character of the PDA@PUF macroscopic support resulted in easy-to-reuse catalysts with minimal leaching into the

liquid medium [40–47]. In particular, $\text{TiO}_2\text{@PDA@PUF}$ foams proved highly efficient and reusable for the depollution of air and water under UV irradiation [41,46].

In this context, we report here our studies toward the immobilisation of eosin Y on an easy-to-prepare and easy-to-handle PDA@PUF support [40–47], which possesses sufficiently large pores to allow efficient light penetration inside the whole three-dimensional structure, as well as efficient transport properties under flow conditions, and which—due to its lightweight and flexibility—can be easily engineered and adapted to any kind of photoreactor [46]. Thanks to the presence of catechol moieties on the surface of the PDA adhesive layer, (3-aminopropyl)triethoxysilane (APTES) was readily anchored on PDA@PUF, resulting in an amination of the surface that allowed the subsequent grafting of eosin Y via an EDC-mediated coupling reaction. The resulting EY-APTES@PDA@PUF material was characterized by ^{29}Si CP-MAS NMR and XPS spectroscopies, ICP-AES and ICP-MS analyses, SEM microscopy, and SEM-EDX elemental mapping, while its catalytic activity was studied for the oxidation of 2-methyl-5-nitroisoquinolin-2-ium iodide to the corresponding isoquinolone [49]. The macroscopic catalyst showed good efficiency and excellent reusability for at least six runs in an easy-to-carry “dip-and-play” mode. Subsequent investigation of the catalytic efficiency of EY-APTES@PDA@PUF for the oxidation of sulfides to sulfoxides [8,29,30,50], however, evidenced non-negligible eosin Y leaching, leading to the progressive deactivation of the catalytic foam in this case. Further studies aimed at exploring alternative synthetic protocols for the preparation of the macroscopic photocatalyst and at solving this issue were next carried out and are additionally described hereafter. In all cases, however, cycling tests also highlighted a relatively fast deactivation of the catalytic foams in sulfide-to-sulfoxide oxidation reactions.

2. Results and Discussion

2.1. Preparation and Characterization of EY-APTES@PDA@PUF Based on Post-Functionalization of PDA@PUF

The first explored strategy for the immobilization of eosin Y on the surface of polydopamine-coated open cell polyurethane foams (PDA@PUF) relied on the previously established proof of concept that a molecular catalyst bearing a pending trialkoxysilyl group can be covalently anchored by condensation of the latter with the catechol groups of the mussel-inspired layer [44]. Thus, after coating a cubic sample of PUF of ca. $2\text{ cm} \times 2\text{ cm} \times 2\text{ cm}$ with a thin layer of PDA by simple immersion in an aqueous solution of dopamine at room temperature buffered at pH 8.5 [40,41], the resulting PDA@PUF material was functionalized with eosin Y in two steps via (i) a silanization process with 3-(triethoxysilyl)propan-1-amine (APTES) in toluene at $70\text{ }^\circ\text{C}$ for 24 h, (ii) an EDC-mediated coupling of the resulting amino-functionalized foam, APTES@PDA@PUF, with eosin Y (Figure 1). Specifically, APTES@PDA@PUF was treated with neutral eosin Y in the presence of 1.5 equiv. of N-hydroxysuccinimide (NHS), and 2 equiv. of EDC hydrochloride in ethanol at room temperature. The successful grafting of eosin Y was visible to the naked eye by a striking colour change from black in APTES@PDA@PUF to red in EY-APTES@PDA@PUF.

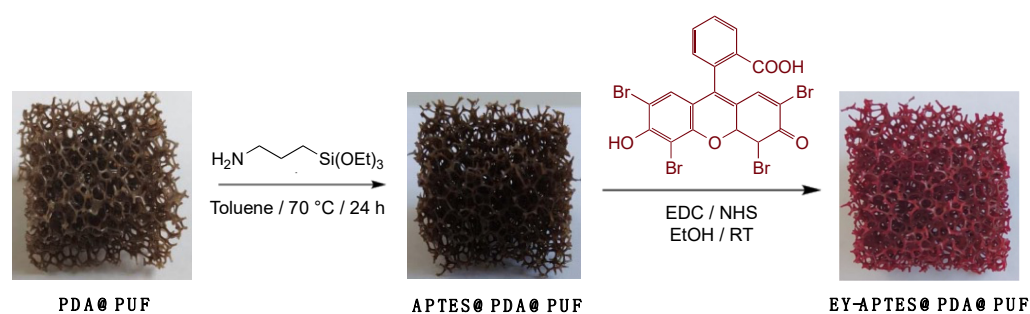


Figure 1. Post-functionalization strategy of PDA@PUF for eosin Y immobilization.

After thorough washing procedures of EY-APTES@PDA@PUF in acetone and CH₃CN/H₂O (1:1), Si and Br contents of 2.544 ± 0.077 g/kg and 1.051 ± 0.029 g/kg were measured by ICP-AES and ICP-MS, respectively. The ²⁹Si CP-MAS NMR spectrum revealed signals between -65.1 ppm and -42.5 ppm (Figure 2), similar to what is observed with APTES@PDA@PUF [51] and what can be seen with covalently anchored APTES on a silica matrix [52]. This shows the presence of T₁, T₂, as well as of cross-linked T₃ + T'₃ and T₄ + T'₄ substructures [53]. Their preservation after the EDC-mediated coupling highlights the robustness of the silicon–catechol bonding formed in the first step of the post-functionalization strategy.

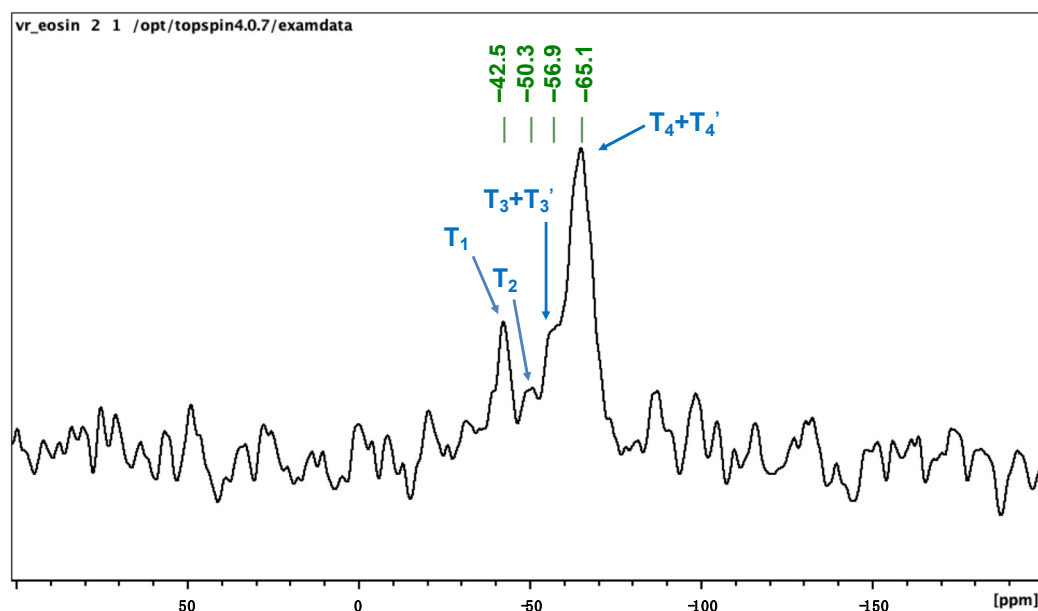


Figure 2. ²⁹Si CP-MAS NMR spectrum of EY-APTES@PDA@PUF.

Low magnification SEM images of EY-APTES@PDA@PUF did not reveal obvious corrugation of the struts' edges (Figure 3), as was previously observed for other PDA@PUF foams functionalized by a molecular catalyst via a similar silanization process [44]. Higher magnification images showed a rough film structure with scattered PDA aggregates, typical of PDA coating on PUF [41]. EDX spectroscopy confirmed the presence of C, N, O, Si, and Br elements on the foam surface (Figure S1), though the latter was not detected on all selected areas, most probably because of its relatively low loading.

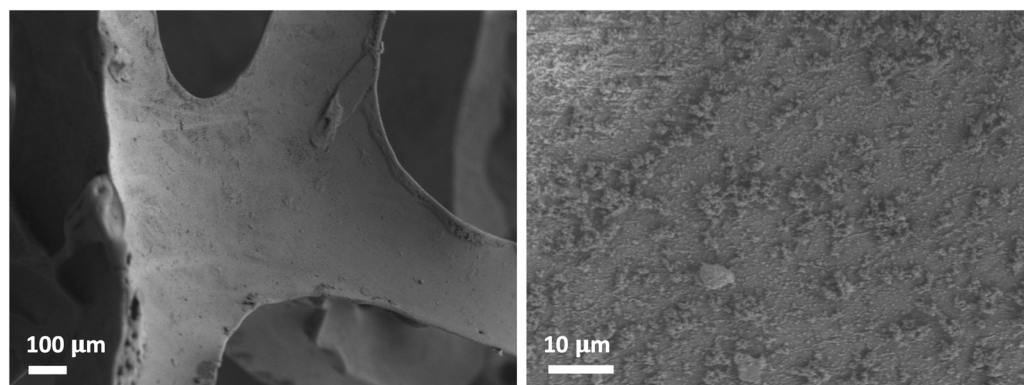


Figure 3. SEM images of as-synthesized EY-APTES@PDA@PUF with different magnifications.

2.2. Photocatalytic Studies

N-Heterocycles containing a pyridine moiety such as quinolines and isoquinolines are privileged scaffolds that occupy key roles in many medicinally related molecules [54].

Similarly, quinolones and isoquinolones exhibit diverse biological and pharmaceutical activities, including anticancer [55], antibiotic [56], antiviral, and antihypertensive activities [57]. It is therefore of interest to develop efficient and practical transformations from readily available quinolines and isoquinolines to quinolones and isoquinolones. In this respect, eosin Y has recently been reported to act as a highly efficient and environmentally friendly homogeneous photocatalyst for the visible-light-mediated aerobic oxidation of *N*-alkylpyridinium salts at room temperature with air as a green oxidant [49]. This reaction thus seemed to be a perfect case study to evaluate the photocatalytic properties of our eosin Y-functionalized foams.

Initial studies focused on the oxidation of 2-methyl-5-nitroisoquinolin-2-ium iodide in the presence of Cs_2CO_3 as base under air at 30–35 °C using eosin Y (2 mol%) or a cubic sample of EY-APTES@PDA@PUF of ca. 2 cm × 2 cm × 2 cm, whose mass was adjusted to have an eosin Y loading of 0.46 mol% as catalysts (Table 1).

Table 1. Optimization of the reaction conditions for the oxidation of 2-methyl-5-nitro-isoquinolin-2-ium iodide under visible light and air using eosin Y or EY-APTES@PDA@PUF as photocatalyst.

Entry	Catalyst	Solvent	Light	Time (h)	Isolated Yield (%)
1 ^a	Eosin Y	THF	40 W CFL	6	94
2 ^b	Eosin Y	THF	24 W white LED	18	71
3 ^b	Eosin Y	EtOH	24 W white LED	18	76
4 ^b	Eosin Y	CH_3CN	24 W white LED	18	96
5 ^c	EY-APTES@PDA@PUF	CH_3CN	24 W white LED	18	70
6 ^d	-	CH_3CN	24 W white LED	18	44

^a Result from [49]: 2-methyl-5-nitro-isoquinolin-2-ium iodide (0.2 mmol), Cs_2CO_3 (0.3 mmol), eosin Y (2 mol%), THF (2 mL), ambient air, 40 W CFL, room temperature. ^b 2-methyl-5-nitro-isoquinolin-2-ium iodide (0.2 mmol), Cs_2CO_3 (0.3 mmol), eosin Y (2 mol%), solvent (2 mL), air balloon, 24 W white LED, ca. 30–35 °C due to LED light heat. ^c 2-methyl-5-nitro-isoquinolin-2-ium iodide (0.2 mmol), Cs_2CO_3 (0.3 mmol), EY-APTES@PDA@PUF (2 cm × 2 cm × 2 cm, 0.46 mol% eosin Y), CH_3CN (8 mL), air balloon, 24 W white LED, ca. 30–35 °C due to LED light heat, 650 rpm. ^d 2-methyl-5-nitro-isoquinolin-2-ium iodide (0.5 mmol), Cs_2CO_3 (0.75 mmol), no catalyst, CH_3CN (20 mL), air balloon, 24 W white LED, ca. 30–35 °C due to LED light heat.

Solvents and light were found to have a prominent influence on the reaction yield. In THF under 24 W white LED light irradiation, the reaction yield achieved 71% after 18 h reaction with eosin Y as catalyst, which was significantly lower than that reported by H. Fu et al. [49] under 40 W compact fluorescent light (CFL) irradiation at room temperature (entry 1 vs. entry 2). Running the reaction in ethanol under otherwise comparable conditions resulted in a similar yield (entry 3), but running it in CH_3CN resulted in a significant improvement, as the expected oxidation product could be isolated in 96% yield after 18 h reaction time (entry 4). The latter conditions were therefore chosen to evaluate the photocatalytic properties of our macroscopic heterogeneous catalyst, with the exception of the solvent volume which had to be increased from 2 to 8 mL in order to allow the complete immersion of the 2 cm × 2 cm × 2 cm foam. Satisfyingly, despite the four-fold decrease of the reactants' concentrations and a little more than a 4-fold decrease of the catalyst loading (0.46 mol% vs. 2 mol%), a 70% isolated yield was obtained after the same reaction time with EY-APTES@PDA@PUF (entry 5). Noteworthy however, 44% yield was obtained in the absence of a photocatalyst under otherwise similar reaction conditions (entry 6), which shows that this reaction can also occur in the absence of a catalyst under these conditions. This reflects the moderate conversion of the related 2-benzylisoquinolin-2-ium bromide to the corresponding isoquinolone that was recently reported in the presence of 1.5 equiv.

of Cs_2CO_3 in DMSO at room temperature [58]. Still, the reaction is 1.6 times faster in the presence of our macroscopic photocatalyst.

Encouraged by these results, we next decided to evaluate the reusability of EY-APTES@PDA@PUF. For that purpose, six consecutive runs of 2-methyl-5-nitro-isoquinolin-2-ium iodide aerobic oxidation under visible light irradiation were conducted with a single sample of freshly prepared EY-APTES@PDA@PUF (2 cm \times 2 cm \times 2 cm, 0.46 mol% EY), that was simply removed from the reaction medium and washed successively with acetone, water, and acetonitrile after each run, before being reused. Satisfyingly, the activity was maintained at the same level for the six runs (Figure 4).

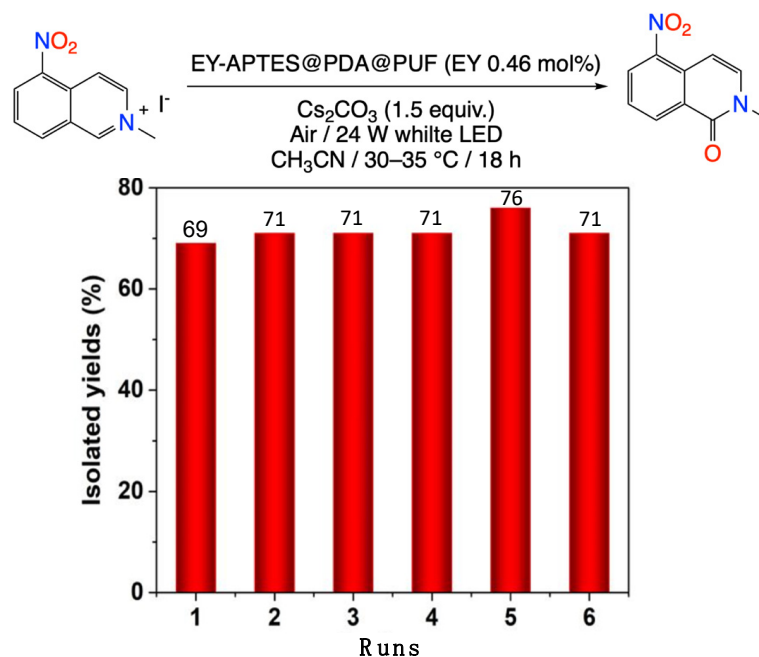


Figure 4. Isolated yields measured over the six successive runs of 2-methyl-5-nitro-isoquinolin-2-ium iodide oxidation photocatalyzed by a single sample of EY-APTES@PDA@PUF. Reaction conditions: 2-methyl-5-nitro-isoquinolin-2-ium iodide (0.2 mmol), Cs_2CO_3 (0.3 mmol), EY-APTES@PDA@PUF (2 cm \times 2 cm \times 2 cm, 0.46 mol% eosin Y), CH_3CN (8 mL), air balloon, 24 W white LED, ca. 30–35 $^\circ\text{C}$ due to LED light heat, 650 rpm.

It is noteworthy however that the reaction media, after each run, were slightly orange coloured, suggesting some eosin Y leaching. Accordingly, the foam became browner (Figure 5) and ICP-AES analysis of the used foam after these six catalytic runs indicated a Si loss of about 22%.



Figure 5. Photograph of the spent EY-APTES@PDA@PUF foam after six cycles of 2-methyl-5-nitro-isoquinolin-2-ium iodide oxidation.

To try to gain some insight on this apparent modification of the foam surface, the spent foam after six cycles of methyl pyridinium salt oxidation was submitted to SEM and SEM-EDX analyses. Low magnification SEM images showed a slight corrugation of the struts' edges, due most probably to repeated solvent swelling in the polymeric foam [44], while higher magnification images revealed a smoother surface with less numerous scattered

PDA aggregates (Figure 6). EDX spectroscopy confirmed the presence of C, N, O, and Si elements on the foam surface but did not show any Br anymore (Figure S2). Adsorbed Cs coming from the used base was detected instead.

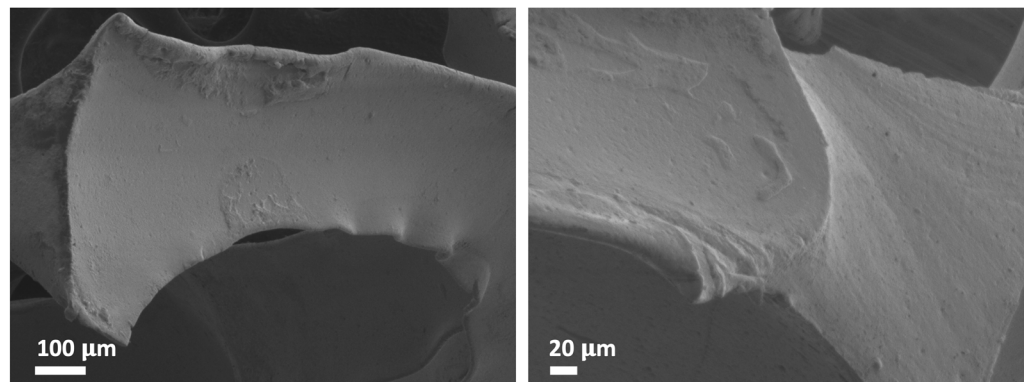


Figure 6. SEM images with different magnifications of spent EY-APTES@PDA@PUF after six cycles of 2-methyl-5-nitro-isoquinolin-2-ium iodide oxidation.

To obtain more insight on the photocatalytic properties of EY-APTES@PDA@PUF and better apprehend the influence of eosin Y leaching on these, we next investigated a reaction of interest where the presence of photocatalyst is absolutely essential for its progress: the selective aerobic oxidation of sulfides to sulfoxides [8,29,30]. Sulfoxides are among the most prevalent and important functional groups found in diverse natural products and pharmaceutical molecules [59]. In addition, sulfoxides are interesting synthetic intermediates for the construction of a vast array of organic compounds [60,61].

Initial studies focused on the oxidation of methyl *p*-tolyl sulfide to its corresponding sulfoxide under 24 W white LED irradiation at 30–35 °C using eosin Y (0.5 mol%) or a cubic sample of EY-APTES@PDA@PUF of ca. 2 cm × 2 cm × 2 cm, whose mass was adjusted to have an eosin Y loading of 0.18 mol%, as catalysts (Table 2). Solvents and air or O₂ atmosphere were found to have a prominent influence on the reaction yield. In CH₃CN/H₂O (3:1) under air, the reaction yield achieved 84% after 6 h reaction with eosin Y as catalyst, giving a turnover number (TON) of 168 and a turnover frequency (TOF) of 28 h^{−1} (entry 1). Running the reaction with EY-APTES@PDA@PUF (0.18 mol% EY) in the same solvent mixture but with 5-fold lower concentration (to allow the complete immersion of the macroscopic catalyst) resulted in only 36% yield after 18 h reaction, thus in a slightly higher TON (200 vs. 168) but a 2.5 slower TOF (entry 2), while running it in pure CH₃CN or CH₃CN/H₂O (1:1) resulted in very low yields, TON and TOF (entries 3 and 4). Satisfyingly however, switching to an O₂ atmosphere and to a 4:1 mixture of CH₃CN/H₂O allowed almost full conversion to be seen after 48 h reaction, reaching a TON of 544 and a TOF of 11.3 h^{−1}. Importantly, the use of a PDA@PUF foam resulted in the absence of reaction (entry 6), showing that PDA by itself is not able to induce the oxidation of sulfides [62].

Interestingly, EY-APTES@PDA@PUF compares well with examples from the literature, where eosin Y has been supported on Amberlite IRA 900 Chloride resin (PSEY, [8]), cotton thread (EY@Cotton thread) [29], and sulfur-doped graphitic carbon nitride (EY-s-g-C₃N₄) [30] and has been used for similar sulfide oxidation reactions under visible-light irradiation and aerobic conditions. These heterogeneous eosin Y catalysts indeed gave lower TON and TOF values (Table 3, entries 2–4 vs. 1).

With the optimized reaction conditions in hand: EY-APTES@PDA@PUF (2 cm × 2 cm × 2 cm, 0.18 mol% EY), CH₃CN/H₂O (4:1) (20 mL), 24 W white LED, O₂ balloon, 30–35 °C, 48 h, recycling tests were then performed with a single sample of freshly prepared EY-APTES@PDA@PUF. In contrast to that observed for the oxidation of 2-methyl-5-nitroisoquinolin-2-ium iodide (Figure 4), a gradual decrease of the NMR yield was observed, from 98% in the 1st run to 59% in the 5th run (Figure 7), which tended to confirm the occurrence of eosin Y leaching. Accordingly, ICP-MS analyses of the used

foam after these five catalytic runs indicated an eosin Y loss of 34% with a Br content of 0.691 ± 0.019 g/kg vs. 1.051 ± 0.029 g/kg in the as-synthesized foam.

Table 2. Optimization of the reaction conditions for the oxidation of methyl *p*-tolyl sulfide under visible light irradiation using eosin Y or EY-APTES@PDA@PUF as photocatalyst ^a.

Entry	Catalyst	Solvent	Time (h)	Yield (%)	TON ^d	TOF (h ⁻¹) ^e
1 ^a	Eosin Y	CH ₃ CN/H ₂ O (3:1)	6	84	168	28
2 ^b	EY-APTES@PDA@PUF	CH ₃ CN/H ₂ O (3:1)	18	36	200	11.1
3 ^b	EY-APTES@PDA@PUF	CH ₃ CN	18	0	0	0
4 ^b	EY-APTES@PDA@PUF	CH ₃ CN/H ₂ O (1:1)	18	9	50	2.8
5 ^c	EY-APTES@PDA@PUF	CH ₃ CN/H ₂ O (4:1)	48	98	544	11.3
6 ^c	PDA@PUF	CH ₃ CN/H ₂ O (4:1)	48	0	0	0

^a Conditions: methyl *p*-tolyl sulfide (1 mmol), eosin Y (0.5 mol%), CH₃CN/H₂O (3:1) (8 mL), 24 W white LED, air balloon, 30–35 °C due to LED light heat. ^b methyl *p*-tolyl sulfide (0.5 mmol), EY-APTES@PDA@PUF (2 cm × 2 cm × 2 cm, 0.18 mol% eosin Y), solvent (20 mL), 24 W white LED, air balloon, 30–35 °C due to LED light heat, 1000 rpm. ^c methyl *p*-tolyl sulfide (0.5 mmol), EY-APTES@PDA@PUF (2 cm × 2 cm × 2 cm, 0.18 mol% eosin Y), CH₃CN/H₂O (4:1) (20 mL), 24 W white LED, O₂ balloon, 30–35 °C due to LED light heat, 1000 rpm. ^d TON expressed as the yield/catalyst loading. ^e TOF (h⁻¹) expressed as the TON/reaction time (h).

Table 3. Oxidation of sulfides under visible light irradiation using eosin Y heterogenized on various supports as photocatalyst.

Entry	Catalyst (EY mol%)	Solvent	Light	Temp.	Atmosph.	R ¹	R ²	Time (h)	Yield (%)	TON ^a	TOF (h ⁻¹) ^b
1 ^c	EY-APTES@PDA@PUF (0.18)	CH ₃ CN/H ₂ O (4:1)	White LED 24 W	30–35 °C	O ₂ balloon	Me	Me	48	98	544	11.3
2 ^d	PSEY (3)	CH ₃ CN/H ₂ O (4:1)	Green LED 3 W	RT	Open air	H	Me	6	91	30.3	5.1
3 ^e	EY@Cotton thread (3.6)	CH ₃ CN/H ₂ O (5:2)	Green light 0.45 mW/cm ²	RT	Air bubbling	H	Me	28	45	12.5	0.4
4 ^f	EY-s-g-C ₃ N ₄	EtOH HCl (0.05 M)	Blue LED	RT	Open air	Cl	C ₆ H ₄ Cl	-	99.6	-	-

^a TON expressed as the yield/catalyst loading. ^b TOF (h⁻¹) expressed as the TON/reaction time (h). ^c This work. ^d Results from ref. [8]. ^e Results from ref. [29]. ^f Results from ref. [30].

A filtration test, run with an as-synthesized EY-APTES@PDA@PUF foam under similar reaction conditions, showed that the *p*-tolyl methyl sulfide oxidation does not stop when the foam is removed from the liquid medium. This unambiguously confirmed that eosin Y was leaching (Figure 8). The reaction rate observed during the 10 h reaction run without the macroscopic photocatalyst even slightly increased compared to that of the first 20 h reaction in the presence of the foam-based catalyst.

Non-negligible adsorption of eosin Y on the PDA layer, possibly linked to a relatively low efficiency of the EDC-mediated coupling reaction with the grafted amine groups, were suspected to be at the origin of this phenomenon. Other strategies for preparing the supported photocatalyst were therefore considered. In a first attempt, in order to have a more efficient eosin-APTES coupling, eosin Y was coupled to APTES prior to the covalent anchoring procedure to PDA@PUF, and this in the presence of COMU instead of EDC to avoid the use of an alcoholic solvent (Figure 9). For that purpose, neutral

eosin Y was reacted with 1.1 equiv. of APTES in the presence of 1.1 equiv. of COMU and 1.1 equiv. of diisopropylethylamine (DIPEA) in dry THF under argon for 30 min at RT. Then a PDA@PUF foam was introduced into the medium and the reaction temperature increased to 50 °C for 24 h. The thus obtained red EY-APTES1@PDA@PUF foam was washed, successively, with acetone, water, and acetonitrile under 24 W white LED irradiation, and dried under vacuum.

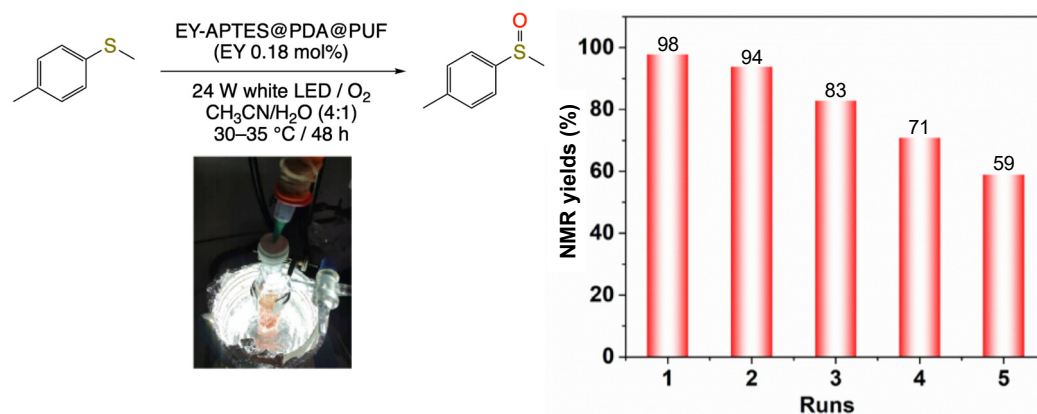


Figure 7. NMR yields measured over five successive runs of *p*-tolyl methyl sulfide oxidation photocatalyzed by a single sample of EY-APTES@PDA@PUF. Reaction conditions: methyl *p*-tolyl sulfide (0.5 mmol), EY-APTES@PDA@PUF (2 cm × 2 cm × 2 cm, 0.18 mol% eosin Y), CH₃CN/H₂O (4:1) (20 mL), 24 W white LED, O₂ balloon, 30–35 °C due to LED light heat, 1000 rpm.

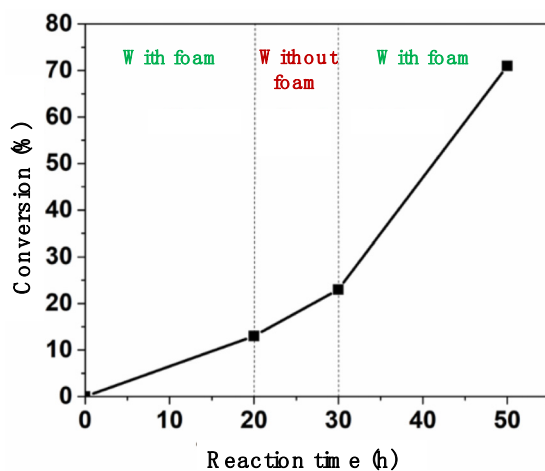


Figure 8. Filtration test on *p*-tolyl methyl sulfide oxidation with EY-APTES@PDA@PUF. Reaction conditions: methyl *p*-tolyl sulfide (0.5 mmol), EY-APTES@PDA@PUF (2 cm × 2 cm × 2 cm, 0.18 mol% EY), CH₃CN/H₂O (4:1) (20 mL), 24 W white LED, O₂ balloon, 30–35 °C, 1000 rpm.



Figure 9. One-pot COMU-mediated eosin-Y-APTES coupling and APTES-PDA condensation for anchoring EY-APTES on PDA@PUF.

Next EY-APTES1@PDA@PUF was tested for the oxidation of *p*-tolyl methyl sulfide in three successive runs under the same conditions that were used for EY-APTES@PDA@PUF. Significant leaching was again observed (Figure 10). While only 24 h reaction was sufficient to reach 97% conversion in the first run, which suggested a higher initial eosin Y loading than with the sequential grafting process, the conversion dropped to 64% after 24 h reaction in the second run and to 49% in the third run. Owing to this severe deactivation, no characterization was carried out.

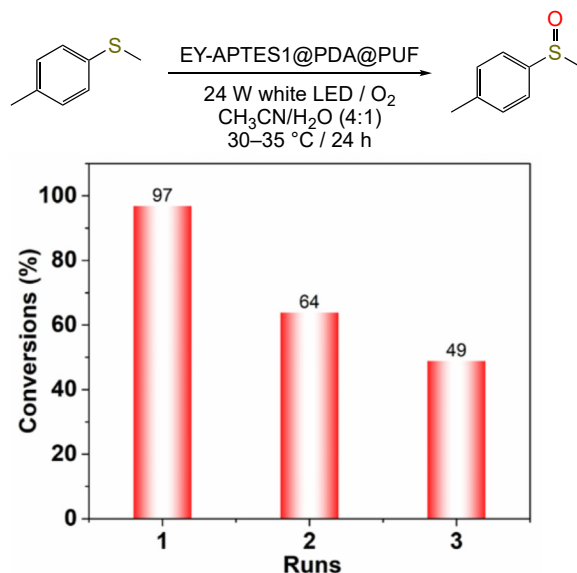
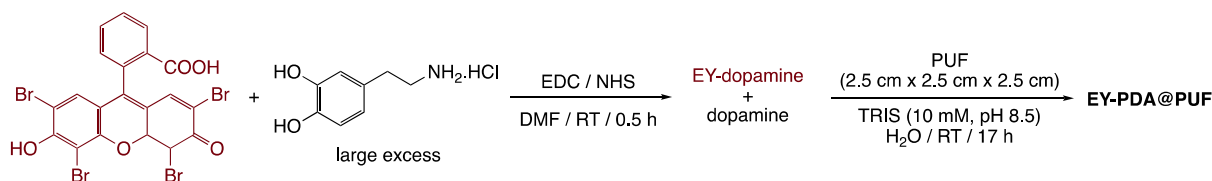


Figure 10. GC conversions measured over three successive runs of *p*-tolyl methyl sulfide oxidation photocatalyzed by a single sample of EY-APTES1@PDA@PUF. Reaction conditions: methyl *p*-tolyl sulfide (0.5 mmol), EY-APTES1@PDA@PUF (1.5 cm × 1.5 cm × 3 cm), CH₃CN/H₂O (4:1) (20 mL), 24 W white LED, O₂ balloon, 30–35 °C due to LED light heat, 1000 rpm.

A completely different strategy was then considered. After an EDC-mediated coupling of eosin Y with dopamine in the presence of a large excess of the latter, the resulting mixture was placed under dopamine self-polymerization conditions to generate an EY-PDA hybrid coating and a cubic sample of PUF (2.5 cm × 2.5 cm × 2.5 cm) was added to provide an EY-PDA@PUF material without APTES (Scheme 1). Following this procedure, the resulting very dark red foam was dried in an oven at 80 °C for 1 h, and then washed with acetone and acetonitrile until the washings were colorless.



Scheme 1. Hybrid EY-PDA coating attempt on PUF.

The catalytic efficiency and reusability of EY-PDA@PUF were then evaluated for the oxidation of thioanisole. Satisfyingly, the conversion of thioanisole to the corresponding sulfoxide reached 99% in only 14 h for the 1st run. However, the conversion decreased to 75% in the 3rd run and this tendency continued until the 5th run with only 20% conversion after 14 h (Figure 11), suggesting considerable eosin Y leaching in this case as well. Furthermore, when EY-PDA@PUF was rinsed under supersonic bath conditions directly after the synthesis, the conversion of thioanisole dropped to 31% in the first run, strongly suggesting that a large amount of adsorbed EY instead of properly grafted EY also existed in this case.

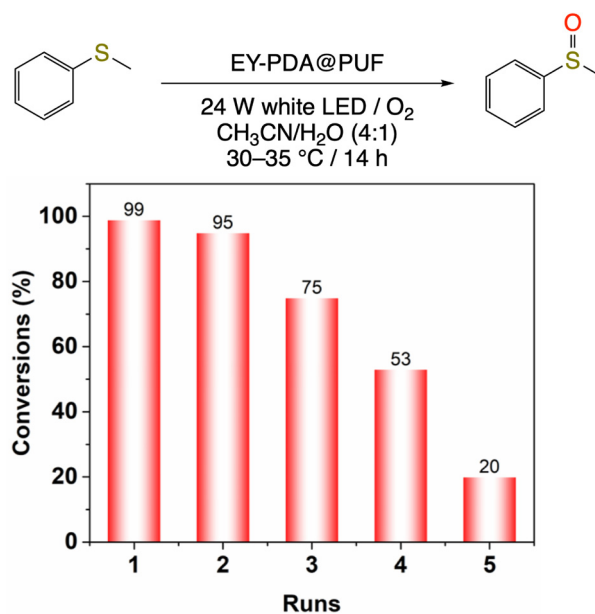


Figure 11. GC conversions measured over five successive runs of thioanisole oxidation photocatalyzed by a single sample of EY-PDA@PUF. Reaction conditions: thioanisole (0.5 mmol), EY-PDA@PUF (2.5 cm × 2.5 cm × 2.5 cm), CH₃CN/H₂O (4:1) (20 mL), 24 W white LED, O₂ balloon, 30–35 °C due to LED light heat, 1000 rpm.

Compared with the previously reported supported EY catalysts [8,16,20,22–32], the stabilities of all our macroscopic PDA@PUF supported catalysts are disappointing, suggesting that PDA may not be an ideal support matrix for eosin Y as non-negligible simple adsorption relative to the expected covalent grafting on the latter seems to have occurred in all of the investigated cases.

3. Experimental Section

3.1. Materials and Methods

Unless otherwise stated, all reagents and solvents were used as provided by commercial suppliers without any further purification/treatment. Polyurethane open cells foams (20 PPI, TCL 40100 soft white reticulated) were given by FoamPartner. Eosin Y (T0035) and 4-(methylthio)toluene (M0949) were purchased from TCI. Dopamine hydrochloride (008896), EDC hydrochloride (024810), N-hydroxysuccinimide (005022), 3-aminopropyltriethoxysilane (ISI0010-98), and thioanisole (002945) were purchased from Fluorochem. Tris base (99.9+%—T1503) was purchased from Sigma-Aldrich. COMU (344284) was provided by Acros Organics. 2-Methyl-5-nitroisoquinolin-2-ium iodide was prepared according to a published procedure [63]. The 18.2 MΩ deionized water (TOC < 1 ppb), supplied by a Q20 Millipore system, was used for the preparation of aqueous solutions and washing procedures with water. RGB LED strip light (Govee, H6190) was manufactured by Shenzhen Intellirocks Tech Co. Ltd. Purifications by column chromatography were carried out with Macherey silica gel (Kieselgel 60). TraceMetal grade HCl 37% (Fisher Scientific) and Rotipuran Supra HNO₃ 69% (Roth) were used for ICP-AES analyses. Element standards were purchased from CPI international.

Scanning electron microscopy (SEM) measurements were recorded with a Hitachi SU8010 FE-SEM microscope at 3 kV at room temperature. No metallization of the samples was performed, but their borders were covered with a metallic tape to evacuate the excess of charge.

Elemental mapping by scanning electron microscopy–energy dispersive X-ray spectroscopy (SEM-EDX) was investigated with a Zeiss Gemini SEM 500 FEG EDAX Octane Elite EDX detector. The X-rays emitted upon electron irradiation were acquired in the range

0–20 keV. Quantification was done using the standard-less ZAF correction method in the Team EDS software from EDAX.

Inductively coupled plasma-atomic emission spectrometry (ICP-AES) and inductively coupled plasma-mass spectrometry (ICP-MS) measurements were performed by the Plateforme Analytique of the Institut Pluridisciplinaire Hubert Curien (UMR CNRS 7178), Strasbourg, France. EY-APTES@PDA@PUF samples were mineralized at 185 °C for 50 min under pressure (Multiwave ECO, Anton Paar), either with HCl (3 mL) for Si loading determination or with HNO₃ (3 mL) for Br loading determination. Blank tests were carried out in parallel under the same conditions. Quantification of Si in the clear obtained solutions was carried out by ICP-AES (Varian 720ES) at two wavelengths: 250.690 nm and 251.611 nm. Quantification of ⁷⁹Br in the clear obtained solutions was conducted using ICP-MS (Agilent 7700) with a standard addition calibration curve to avoid matrix effects observed with an external calibration.

Gas chromatographic (GC) analyses were conducted on a GC Agilent with FID detectors using Agilent HP1 column (30 m, 0.35 mm, 0.25 μm), with hydrogen as gas carrier and with tetradecane as the internal standard. The retention times and GC responses in terms of area versus concentration of the reagents and products were calibrated by using pure components directly transferred from reactive solutions. The conversion and product distribution were calculated from the GC results.

Solution NMR spectra were recorded at 298 K on a Bruker Avance III HD 400 MHz spectrometer operating at 400.13 MHz for ¹H. The chemical shifts are referenced to the residual deuterated. Chemical shifts (δ) are expressed in ppm (see the Supporting Information).

For solid-state NMR spectra, the foam samples were frozen into N_{2(l)} and ground. The ground foams were then packed in 4 mm ZrO₂ rotors under air. The ²⁹Si CP-MAS experiment spectra were recorded at 298 K on a Bruker Solid State DSX 300 MHz NMR spectrometer operating at 69.66 MHz, and equipped with a Bruker 4 mm ¹H/X CP-MAS probe. A shaped cross-polarization pulse sequence with tangential modulation on both channels was used with the following parameters: the spinning speed was set to 10 kHz, the spectral width to 30 kHz, the contact time was in the range of 1 ms, the proton RF field was around 55 kHz for decoupling (using SPINAL 64 sequence) and 40 kHz for contact, and with a recycle delay of 5 s. The spectra were calibrated with respect an external PDMS sample (−35.1 ppm).

3.2. Experimental Procedures

3.2.1. Open Cell Polyurethane Foam (PUF) Coating with Polydopamine (PDA)

The used procedure was similar to our previously reported procedures [40,41]. Dopamine hydrochloride (2 mg/mL) was dissolved in an aqueous solution (500 mL) of Tris base (10 mM) buffered to pH 8.5 with aqueous HCl (1 M). Four samples of PUF (ca. 2 cm × 2 cm × 2 cm or 1.5 cm × 1.5 cm × 3 cm) were immersed in the stirred solution for 17 h at RT. The reaction medium slowly turned black. The resulting PDA-coated PUF samples (PDA@PUF) were then taken out of the medium, dried in an oven at 80 °C for 1.5 h, washed in vigorously stirred water (3 × 10 min in 500 mL) and dried again in an oven at 80 °C.

3.2.2. Functionalization of PDA@PUF with APTES

A cubic sample of PDA@PUF (ca. 2 cm × 2 cm × 2 cm) was washed in vigorously stirred toluene (3 × 25 mL) at room temperature for several minutes and dried under vacuum prior to the functionalization.

A stirring bar and the sample of PDA@PUF were introduced in a Schlenk tube under argon. This was followed by the additions of freshly distilled toluene (25 mL) and APTES (0.23 mL, 1 mmol). After 24 h of stirring at 70 °C, the resulting APTES-functionalized foam, APTES@PDA@PUF, was removed from the reaction medium, washed for a few minutes in vigorously stirred toluene (3 × 25 mL), and then dried under vacuum.

3.2.3. Coupling of Eosin Y with APTES@PDA@PUF

A stirring bar was introduced in a Schlenk tube. This was followed by the additions of ethanol (20 mL), eosin Y (65 mg, 0.1 mmol), N-hydroxysuccinimide (17 mg, 0.15 mmol), and EDC hydrochloride (38 mg, 0.2 mmol) in this order. After 0.5 h of stirring, the cubic sample of APTES@PDA@PUF was then immersed into the solution for overnight stirring at room temperature. The resulting eosin Y-coupled foam, EY-APTES@PDA@PUF, was then washed in acetone (10 × 60 mL) and CH₃CN/H₂O (4:1) (2 × 60 mL) and dried under vacuum.

EY-APTES@PDA@PUF was characterized by SEM, EDX, ²⁹Si CP-MAS NMR, ICP-AES, revealing mean Si contents of 2.544 ± 0.077 g/kg and ICP-MS, revealing mean Br contents of 1.051 ± 0.029 g/kg.

3.2.4. Preparation of EY-APTES1@PDA@PUF in a One-Pot Procedure from PDA@PUF

A stirring bar, neutral eosin Y (324 mg, 0.50 mmol) and COMU (235 mg, 0.55 mmol) were introduced in a Schlenk tube under vacuum argon. Freshly distilled THF (25 mL), N,N-diisopropylethylamine (0.12 mL, 0.75 mmol), and APTES (0.26 mL, 0.55 mmol) were subsequently added, and the mixture stirred for 30 min at room temperature. A sample of PDA@PUF (ca. 1.5 cm × 1.5 cm × 3 cm) was then immersed into the solution and the mixture was stirred for 24 h under argon at 50 °C. The resulting EY-APTES1@PDA@PUF foam was washed overnight (each time) under vigorous stirring in acetone (60 mL), H₂O (60 mL) and CH₃CN (60 mL) under 24 W white LED irradiation, and then dried under vacuum.

3.2.5. Preparation of EY-PDA@PUF

A 25 mL round-bottomed flask was charged with eosin Y (50 mg, 0.08 mmol), N-hydroxysuccinimide (10 mg, 0.08 mmol), EDC hydrochloride (16 mg, 0.08 mmol), and DMF (5 mL). After 10 min of stirring at room temperature, dopamine hydrochloride (250 mg, 1.32 mmol) was added, and the mixture was reacted for 30 min at the same temperature. The reaction mixture was then poured into a beaker containing an aqueous solution (125 mL) of Tris base (10 mM) buffered to pH 8.5 with aqueous HCl (1 M). A cubic sample of pristine PUF (ca. 2.5 cm × 2.5 cm × 2.5 cm) was immersed in the beaker and the reaction mixture stirred for 17 h at room temperature. The resulting very dark red EY-PDA@PUF foam was then taken out from the beaker and dried in an oven at 80 °C for 1 h. This was followed by thorough washings under vigorous stirring in acetone (60 mL) and CH₃CN (60 mL) and drying under vacuum.

3.2.6. General Procedure for the Oxidation of 2-methyl-5-nitro-isoquinolin-2-ium Iodide Photocatalyzed by EY-APTES@PDA@PUF

A stirring bar and a cubic sample of EY-APTES@PDA@PUF of ca. 2 cm × 2 cm × 2 cm, whose mass (280 mg) was adjusted in function of its Br content established by ICP-AES (0.105 wt%) to have an eosin Y loading of 0.925 μmol, were introduced in a 10 mL Schlenk tube.

2-Methyl-5-nitroisoquinolin-2-ium iodide (0.2 mmol), Cs₂CO₃ (0.3 mmol), and acetonitrile (8 mL) were then added so that the foam was totally immersed. The tube was sealed with a rubber septum equipped with an air balloon, and the reaction mixture stirred at room temperature (650 rpm) under irradiation with a 24 W white LED strip for 24 h. Water (8 mL) was then added, and the product was extracted with ethyl acetate (8 mL × 2). After purification by chromatography on silica (petroleum ether/ethyl acetate, 1:1) and solvent removal, the oxidation product, obtained as a yellow solid, was weighed to determine the yield, and its identity confirmed by ¹H NMR in CD₃CN.

3.2.7. General Procedures for the Oxidation of Sulfides to Sulfoxides Photocatalyzed by EY-APTES@PDA@PUF, EY-APTES1@PDA@PUF or EY-PDA@PUF

A stirring bar and a sample of EY-APTES@PDA@PUF of ca. 2 cm × 2 cm × 2 cm, EY-APTES1@PDA@PUF of ca. 1.5 cm × 1.5 cm × 3 cm, or EY-PDA@PUF of ca. 2.5 cm × 2.5 cm × 2.5 cm were introduced in a 50 mL Schlenk tube. The mass (280 mg) of

EY-APTES@PDA@PUF was adjusted as a function of its Br content established by ICP- AES (0.105 wt%) to have an eosin Y loading of 0.925 μmol .

Acetonitrile/water (4:1) (20 mL) was then added to immerse the foam. This was followed by the addition of *p*-tolyl methyl sulfide (with EY-APTES@PDA@PUF or EY-APTES1@PDA@PUF as catalyst) or thioanisole (with EY-PDA@PUF as catalyst) (0.5 mmol). The tube was then sealed with a rubber septum, the atmosphere quickly evacuated and refilled with O₂ several times, and finally equipped with an O₂ balloon. The reaction mixture was vigorously stirred (1000 rpm) at room temperature and aliquots of the reaction medium (50 μL) were periodically removed by syringe to determine the conversion by GC analysis or ¹H NMR spectroscopy. The aliquots were diluted with acetone (3 mL) for GC analysis or dried under vacuum and re-dissolved in CDCl₃ s for ¹H NMR spectroscopy.

3.2.8. Reusability Procedure

After each run, the foam was separated from the liquid then washed with acetone (3 \times 30 mL), H₂O (3 \times 30 mL), and acetonitrile (3 \times 30 mL), dried under vacuum, and re-used as described above.

3.2.9. Filtration Test for the Oxidation of *p*-Tolyl Methyl Sulfide

In this control experiment conducted for checking the occurrence of eosin Y leaching into the liquid medium, the above-described general procedure for the oxidation of sulfides to sulfoxides was followed using *p*-tolyl methyl sulfide (0.5 mmol) in CH₃CN/H₂O (4:1) (20 mL), an O₂ balloon, a 24 W white LED strip, and a cubic sample of EY-APTES@PDA@PUF of ca. 2 cm \times 2 cm \times 2 cm, whose mass (280 mg) was adjusted as a function of its Br content established by ICP-AES (0.105 wt%) to have an EY loading of 0.925 μmol , as catalyst, except that, after 20 h reaction, the EY-APTES@PDA@PUF foam was removed from the reaction medium for 10 h. Then, EY-APTES@PDA@PUF was reintroduced in the reacting vessel for 20 h. During the whole process, the O₂ atmosphere was maintained. The course of the reaction was monitored by sampling the reaction medium at T = 20, 30, and 50 h, and analyzing the removed aliquots (50 μL) by GC.

4. Conclusions

In summary, we prepared EY-APTES@PDA@PUF, EY-APTES1@PDA@PUF and PDA-EY@PUF foams that functioned as photocatalysts for the aerobic oxidation of an N-methylisoquinolinium salt to the corresponding isoquinolone and/or of sulfides to sulfoxides under visible-light irradiation. Following a simple dip-coating protocol of PUF into an aqueous solution of dopamine, buffered to a pH of 8.5, the resulting PDA@PUF macroscopic material was functionalized with eosin Y. This was carried out either via a two-step process involving silanization with APTES and EDC-mediated coupling with eosin Y, or via a one-pot protocol implying the coupling of eosin Y with APTES prior to the covalent anchoring procedure by condensation of the alkoxy silane groups on the catechol moieties of PDA. Alternatively, a one-step coating-functionalization strategy implying the direct coupling of eosin Y with dopamine was adopted to generate EY-PDA@PUF. All three macroscopic photocatalyst showed high efficiency for their first use in a model of sulfide-to-sulfoxide oxidation reaction. However, cycling tests highlighted fast deactivation due to significant eosin Y leaching. This was clearly demonstrated in the case of EY-APTES@PDA@PUF by a filtration test and ICP-MS measurements that showed a 34% eosin Y loss after five catalytic runs. Non-negligible simple adsorption of eosin Y on the PDA adhesive layer, relatively to the expected covalent anchoring, is suspected to be the origin of this phenomenon.

Supplementary Materials: The following supporting information can be downloaded at <https://www.mdpi.com/article/10.3390/catal13030589/s1>. Figure S1: EDX spectrum of as-synthesized EY-APTES@PDA@PUF. Figure S2: EDX spectrum of spent EY-APTES@PDA@PUF after 6 cycles of 2-methyl-5-nitro-isoquinolinium iodide oxidation. Figure S3: ¹H NMR (CD₃CN) spectrum of 2-methyl-5-nitro-isoquinolone. Figure S4: ¹H NMR (CDCl₃) spectrum of *p*-tolyl methyl sulfoxide.

Figure S5: ^1H NMR (CDCl_3) spectrum of a crude reaction mixture of *p*-tolyl methyl sulfide oxidation. ICP-AES and ICP-MS analyses report for as-synthesized and spent EY-APTES@PDA@PUF.

Author Contributions: Investigation, H.P., T.R. and P.B.; funding acquisition, V.R.; supervision: V.R.; writing—original draft preparation, H.P.; writing—review and editing, V.R. All authors have read and agreed to the published version of the manuscript.

Funding: This work was supported by the University of Strasbourg (IdEx 2019—Contrats doctoraux). H.P. thanks the International Doctoral Program of the Université de Strasbourg for his PhD fellowship.

Data Availability Statement: The data presented in this study are available on request from the corresponding author.

Acknowledgments: The authors thank the NMR and Analytical Platform managers of LIMA, Emeric Wasielewski and Matthieu Chesse, who contributed, by their valuable technical support, to the completion of this research project. Anne Boos and Pascale Ronot from the IPHC (UMR CNRS 7178) are gratefully acknowledged for carrying out the ICP-AES and ICP-MS measurements. All authors have read and agreed to the published version of the proofs.

Conflicts of Interest: The authors declare no conflict of interest.

References

1. Hari, D.P.; König, B. Synthetic applications of eosin Y in photoredox catalysis. *Chem. Commun.* **2014**, *50*, 6688–6699. [[CrossRef](#)]
2. Pitre, S.P.; McTiernan, C.D.; Ismaili, H.; Scaiano, J.C. Mechanistic Insights and Kinetic Analysis for the Oxidative Hydroxylation of Arylboronic Acids by Visible Light Photoredox Catalysis: A Metal-Free Alternative. *J. Am. Chem. Soc.* **2013**, *135*, 13286–13289. [[CrossRef](#)] [[PubMed](#)]
3. Huang, L.; Zhao, J.; Guo, S.; Zhang, C.; Ma, J. Bodipy Derivatives as Organic Triplet Photosensitizers for Aerobic Photoorganocatalytic Oxidative Coupling of Amines and Photooxidation of Dihydroxynaphthalenes. *J. Org. Chem.* **2013**, *78*, 5627–5637. [[CrossRef](#)]
4. Romero, N.A.; Nicewicz, D.A. Organic Photoredox Catalysis. *Chem. Rev.* **2016**, *116*, 10075–10166. [[CrossRef](#)]
5. Yan, J.; Tang, H.; Kuek, E.J.R.; Shi, X.; Liu, C.; Zhang, M.; Piper, J.L.; Duan, S.; Wu, J. Divergent functionalization of aldehydes photocatalyzed by neutral eosin Y with sulfone reagents. *Nat. Commun.* **2021**, *12*, 7214. [[CrossRef](#)]
6. Herbrik, F.; Camarero González, P.; Krstic, M.; Puglisi, A.; Benaglia, M.; Sanz, M.A.; Rossi, S. Eosin Y: Homogeneous Photocatalytic In-Flow Reactions and Solid-Supported Catalysts for In-Batch Synthetic Transformations. *Appl. Sci.* **2020**, *10*, 5596. [[CrossRef](#)]
7. Yang, X.-J.; Chen, B.; Zheng, L.-Q.; Wu, L.-Z.; Tung, C.-H. Highly efficient and selective photocatalytic hydrogenation of functionalized nitrobenzenes. *Green Chem.* **2014**, *16*, 1082–1086. [[CrossRef](#)]
8. Sridhar, A.; Rangasamy, R.; Selvaraj, M. Polymer-supported eosin Y as a reusable photocatalyst for visible light mediated organic transformations. *New J. Chem.* **2019**, *43*, 17974–17979. [[CrossRef](#)]
9. Rueping, M.; Zhu, S.; Koenigs, R.M. Photoredox catalyzed C–P bond forming reactions—Visible light mediated oxidative phosphorylations of amines. *Chem. Commun.* **2011**, *47*, 8679–8681. [[CrossRef](#)] [[PubMed](#)]
10. Mangi, F.; Abdul Sattar, F.; Lu, C.Z. Metal Free Synthesis of Organosulfur Compounds Employing Eosin Y as Photoredox Catalyst. *Chem. Methodol.* **2019**, *3*, 535–542. [[CrossRef](#)]
11. Hari, D.P.; Schroll, P.; König, B. Metal-Free, Visible-Light-Mediated Direct C–H Arylation of Heteroarenes with Aryl Diazonium Salts. *J. Am. Chem. Soc.* **2012**, *134*, 2958–2961. [[CrossRef](#)]
12. Cantillo, D.; de Frutos, O.; Rincón, J.A.; Mateos, C.; Kappe, C.O. Continuous Flow α -Trifluoromethylation of Ketones by Metal-Free Visible Light Photoredox Catalysis. *Org. Lett.* **2014**, *16*, 896–899. [[CrossRef](#)] [[PubMed](#)]
13. Pham, P.V.; Nagib, D.A.; MacMillan, D.W.C. Photoredox Catalysis: A Mild, Operationally Simple Approach to the Synthesis of α -Trifluoromethyl Carbonyl Compounds. *Angew. Chem. Int. Ed.* **2011**, *50*, 6119–6122. [[CrossRef](#)] [[PubMed](#)]
14. Xu, J.; Shanmugam, S.; Duong, H.T.; Boyer, C. Organo-photocatalysts for photoinduced electron transfer-reversible addition–fragmentation chain transfer (PET-RAFT) polymerization. *Polym. Chem.* **2015**, *6*, 5615–5624. [[CrossRef](#)]
15. Yeow, J.; Chapman, R.; Xu, J.; Boyer, C. Oxygen tolerant photopolymerization for ultralow volumes. *Polym. Chem.* **2017**, *8*, 5012–5022. [[CrossRef](#)]
16. Shanmugam, S.; Xu, S.; Adnan, N.N.M.; Boyer, C. Heterogeneous Photocatalysis as a Means for Improving Recyclability of Organocatalyst in “Living” Radical Polymerization. *Macromolecules* **2018**, *51*, 779–790. [[CrossRef](#)]
17. Neumann, M.; Földner, S.; König, B.; Zeitler, K. Metal-Free, Cooperative Asymmetric Organophotoredox Catalysis with Visible Light. *Angew. Chem. Int. Ed.* **2011**, *50*, 951–954. [[CrossRef](#)] [[PubMed](#)]
18. Neumann, M.; Zeitler, K. A Cooperative Hydrogen-Bond-Promoted Organophotoredox Catalysis Strategy for Highly Diastereoselective, Reductive Enone Cyclization. *Chem. Eur. J.* **2013**, *19*, 6950–6955. [[CrossRef](#)]
19. Nicewicz, D.A.; MacMillan, D.W.C. Merging Photoredox Catalysis with Organocatalysis: The Direct Asymmetric Alkylation of Aldehydes. *Science* **2008**, *322*, 77–80. [[CrossRef](#)]

20. Herbrink, F.; Rossi, S.; Sanz, M.; Puglisi, A.; Benaglia, M. Immobilised eosin Y for the photocatalytic oxidation of tetrahydroisoquinolines in flow. *ChemCatChem* **2022**, *14*, e202200461. [CrossRef]
21. Douglas, J.J.; Sevrin, M.J.; Stephenson, C.R.J. Visible Light Photocatalysis: Applications and New Disconnections in the Synthesis of Pharmaceutical Agents. *Org. Proc. Res. Dev.* **2016**, *20*, 1134–1147. [CrossRef]
22. Mou, Z.; Dong, Y.; Li, S.; Du, Y.; Wang, X.; Yang, P.; Wang, S. Eosin Y functionalized graphene for photocatalytic hydrogen production from water. *Int. J. Hydrogen Energy* **2011**, *36*, 8885–8893. [CrossRef]
23. Wang, J.; Liu, Y.; Li, Y.; Xia, L.; Jiang, M.; Wu, P. Highly Efficient Visible-Light-Driven H₂ Production via an Eosin Y-Based Metal–Organic Framework. *Inorg. Chem.* **2018**, *57*, 7495–7498. [CrossRef] [PubMed]
24. Kumar, G.; Solanki, P.; Nazish, M.; Neogi, S.; Kureshy, R.I.; Khan, N.-u.H. Covalently hooked EOSIN-Y in a Zr(IV) framework as visible-light mediated, heterogeneous photocatalyst for efficient CH functionalization of tertiary amines. *J. Catal.* **2019**, *371*, 298–304. [CrossRef]
25. Yu, X.; Yang, Z.; Qiu, B.; Guo, S.; Yang, P.; Yu, B.; Zhang, H.; Zhao, Y.; Yang, X.; Han, B.; et al. Eosin Y-Functionalized Conjugated Organic Polymers for Visible-Light-Driven CO₂ Reduction with H₂O to CO with High Efficiency. *Angew. Chem. Int. Ed.* **2019**, *58*, 632–636. [CrossRef]
26. Zhao, Y.; Shao, S.; Xia, J.; Huang, Y.; Zhang, Y.C.; Li, X.; Cai, T. Hydrophilic ultrafiltration membranes with surface-bound eosin Y for an integrated synthesis-separation system of aqueous RAFT photopolymerization. *J. Mater. Chem. A* **2020**, *8*, 9825–9831. [CrossRef]
27. Wang, C.-A.; Li, Y.-W.; Cheng, X.-L.; Zhang, J.-P.; Han, Y.-F. Eosin Y dye-based porous organic polymers for highly efficient heterogeneous photocatalytic dehydrogenative coupling reaction. *RSC Adv.* **2017**, *7*, 408–414. [CrossRef]
28. Teixeira, R.I.; de Lucas, N.C.; Garden, S.J.; Lanterna, A.E.; Scaiano, J.C. Glass wool supported ruthenium complexes: Versatile, recyclable heterogeneous photoredox catalysts. *Catal. Sci. Technol.* **2020**, *10*, 1273–1280. [CrossRef]
29. Chu, Y.; Huang, Z.; Liu, R.; Boyer, C.; Xu, J. Scalable and Recyclable Heterogeneous Organo-photocatalysts on Cotton Threads for Organic and Polymer Synthesis. *ChemPhotoChem* **2020**, *4*, 5201–5208. [CrossRef]
30. Singh, P.; Yadav, R.K.; Kumar, K.; Lee, Y.; Gupta, A.K.; Kumar, K.; Yadav, B.C.; Singh, S.N.; Dwivedi, D.K.; Nam, S.-H.; et al. Eosin-Y and sulfur-codoped g-C₃N₄ composite for photocatalytic applications: The regeneration of NADH/NADPH and the oxidation of sulfide to sulfoxide. *Catal. Sci. Technol.* **2021**, *11*, 6401–6410. [CrossRef]
31. Li, P.; Wang, G.-W.; Zhu, X.; Wang, L. Magnetic nanoparticle-supported eosin Y ammonium salt: An efficient heterogeneous catalyst for visible light oxidative C–C and C–P bond formation. *Tetrahedron* **2019**, *75*, 3448–3455. [CrossRef]
32. Jarrahi, M.; Maleki, B.; Tayebee, R. Magnetic nanoparticle-supported eosin Y salt [SB-DABCO@eosin] as an efficient heterogeneous photocatalyst for the multi-component synthesis of chromeno [4,3-b]chromene in the presence of visible light. *RSC Adv.* **2022**, *12*, 28886–28901. [CrossRef]
33. Bakker, J.J.; Groendijk, W.J.; de Lathouder, K.M.; Kapteijn, F.; Moulijn, J.A.; Kreutzer, M.T.; Wallin, S.A. Enhancement of catalyst performance using pressure pulses on macroporous structured catalysts. *Ind. Eng. Chem. Res.* **2007**, *46*, 8574–8583. [CrossRef]
34. Giani, L.; Groppi, G.; Tronconi, E. Mass-transfer characterization of metallic foams as supports for structured catalysts. *Ind. Eng. Chem. Res.* **2005**, *44*, 4993–5002. [CrossRef]
35. Richardson, J.; Peng, Y.; Remue, D. Properties of ceramic foam catalyst supports: Pressure drop. *Appl. Catal. A* **2000**, *204*, 19–32. [CrossRef]
36. Lacroix, M.; Nguyen, P.; Schweich, D.; Pham-Huu, C.; Savin-Poncet, S.; Edouard, D. Pressure drop measurements and modeling on SiC foams. *Chem. Eng. Sci.* **2007**, *62*, 3259–3267. [CrossRef]
37. Lacroix, M.; Dreibine, L.; de Tymowski, B.; Vigneron, F.; Edouard, D.; Bégin, D.; Nguyen, P.; Pham, C.; Savin-Poncet, S.; Luck, F.; et al. Silicon carbide foam composite containing cobalt as a highly selective and re-usable Fischer–Tropsch synthesis catalyst. *Appl. Catal. A* **2011**, *397*, 62–72. [CrossRef]
38. Engels, H.W.; Pirkel, H.G.; Albers, R.; Albach, R.W.; Krause, J.; Hoffmann, A.; Casselmann, H.; Dormish, J. Polyurethanes: Versatile materials and sustainable problem solvers for today’s challenges. *Angew. Chem. Int. Ed.* **2013**, *52*, 9422–9441. [CrossRef]
39. Lee, H.; Dellatore, S.M.; Miller, W.M.; Messersmith, P.B. Mussel-inspired surface chemistry for multifunctional coatings. *Science* **2007**, *318*, 426–430. [CrossRef]
40. Edouard, D.; Ritleng, V.; Jierry, L.; Chau, N.T.T. Method for Modifying the Surface Properties of Elastomer Cellular Foams. WO 2016012689A2, 2016. Available online: <https://patents.google.com/patent/WO2016012689A3/en> (accessed on 23 February 2023).
41. Pardieu, E.; Chau, N.T.T.; Dintzer, T.; Romero, T.; Favier, D.; Roland, T.; Edouard, D.; Jierry, L.; Ritleng, V. Polydopamine-coated open cell polyurethane foams as an inexpensive, flexible yet robust catalyst support: A proof of concept. *Chem. Commun.* **2016**, *52*, 4691–4693. [CrossRef]
42. Lefebvre, L.; Kelber, J.; Jierry, L.; Ritleng, V.; Edouard, D. Polydopamine-coated open cell polyurethane foam as an efficient and easy-to-regenerate soft structured catalytic support (S2CS) for the reduction of dye. *J. Environ. Chem. Eng.* **2017**, *5*, 79–85. [CrossRef]
43. Lefebvre, L.; Kelber, J.; Mao, X.; Ponzio, F.; Agusti, G.; Vigier-Carrière, C.; Ball, V.; Jierry, L.; Ritleng, V.; Edouard, D. Borohydride-functionalized polydopamine-coated open cell polyurethane foam as a reusable soft structured material for reduction reactions: Application to the removal of a dye. *Environ. Prog. Sustain. Energy* **2019**, *38*, 329–335. [CrossRef]

44. Ait Khouya, A.; Mendez Martinez, M.L.; Bertani, P.; Romero, T.; Favier, D.; Roland, T.; Guidal, V.; Bellière-Baca, V.; Edouard, D.; Jierry, L.; et al. Coating of polydopamine on polyurethane open cell foams to design soft structured supports for molecular catalysts. *Chem. Commun.* **2019**, *55*, 11960–11963. [[CrossRef](#)]
45. Birba, L.; Ritleng, V.; Jierry, L.; Agusti, G.; Fongarland, P.; Edouard, D. An efficient bio-inspired catalytic tool for hydrogen release at room temperature from a stable borohydride solution. *Int. J. Energy Res.* **2020**, *44*, 10612–10627. [[CrossRef](#)]
46. Ponzio, F.; Kelber, J.; Birba, L.; Rekab, K.; Ritleng, V.; Jierry, L.; Edouard, D. Polydopamine film coating on polyurethane foams as efficient “sunscreen”. Application to photocatalysis under UV irradiation. *Environ. Technol. Innov.* **2021**, *23*, 101618. [[CrossRef](#)]
47. Peng, H.; Zhang, X.; Papaefthimiou, V.; Pham-Huu, C.; Ritleng, V. Pd-functionalized polydopamine-coated polyurethane foam: A readily prepared and highly reusable structured catalyst for selective alkyne semi-hydrogenation and Suzuki coupling under air. *Green Chem.* **2023**, *25*, 264–279. [[CrossRef](#)]
48. Saiz-Poseu, J.; Mancebo-Aracil, J.; Nador, F.; Busqué, F.; Ruiz-Molina, D. The chemistry behind catechol-based adhesion. *Angew. Chem. Int. Ed.* **2019**, *58*, 696–714. [[CrossRef](#)]
49. Jin, Y.; Ou, L.; Yang, H.; Fu, H. Visible-Light-Mediated Aerobic Oxidation of N-Alkylpyridinium Salts under Organic Photocatalysis. *J. Am. Chem. Soc.* **2017**, *139*, 14237–14243. [[CrossRef](#)]
50. Sandaroos, R.; Maleki, B.; Naderi, S.; Peiman, S. Efficient synthesis of sulfones and sulfoxides from sulfides by cobalt-based. Schiff complex supported on nanocellulose as catalyst and Oxone as the terminal oxidant. *Inorg. Chem. Commun.* **2023**, *148*, 110294. [[CrossRef](#)]
51. Peng, H. Supports Catalytiques Structurés à Base de Mousses de Polyuréthane Fonctionnalisées: Applications en Photocatalyse et en Semi-hydrogénation D’alcynes. Ph.D. Thesis, Université de Strasbourg, Strasbourg, France, 2023.
52. Vejayakumaran, P.; Rahman, I.A.; Sipaut, C.S.; Ismail, J.; Chee, C.K. Structural and thermal characterizations of silica nanoparticles grafted with pendant maleimide and epoxide groups. *J. Colloid Interface Sci.* **2008**, *328*, 81–91. [[CrossRef](#)]
53. Albert, K.; Pflleiderer, B.; Bayer, E.; Schnabel, R. Characterization of chemically modified glass surfaces by ¹³C and ²⁹Si CP/MAS NMR spectroscopy. *J. Colloid Interface Sci.* **1991**, *142*, 35–40. [[CrossRef](#)]
54. Carey, J.S.; Laffan, D.; Thomson, C.; Williams, M.T. Analysis of the reactions used for the preparation of drug candidate molecules. *Org. Biomol. Chem.* **2006**, *4*, 2337–2347. [[CrossRef](#)]
55. Claassen, G.; Brin, E.; Crogan-Grundy, C.; Vaillancourt, M.T.; Zhang, H.Z.; Cai, S.X.; Drewe, J.; Tseng, B.; Kasibhatla, S. Selective activation of apoptosis by a novel set of 4-aryl-3-(3-aryl-1-oxo-2-propenyl)-2(1H)-quinolinones through a Myc-dependent pathway. *Cancer Lett.* **2009**, *274*, 243–249. [[CrossRef](#)]
56. Forbis, R.M.; Rinehart, K.L. Nybomycin. VII. Preparative routes to nybomycin and deoxynybomycin. *J. Am. Chem. Soc.* **1973**, *95*, 5003–5013. [[CrossRef](#)]
57. Afonso, A.; Weinstein, J.; Gentles, M.J. Antiviral Compounds and Antihypertensive Compounds. Patent WO92004327, 19 March 1992.
58. Bai, L.-G.; Zhou, Y.; Zhuang, X.; Zhang, L.; Xue, J.; Lin, X.-L.; Cai, T.; Luo, Q.-L. Base-promoted aerobic oxidation of N-alkyl iminium salts derived from isoquinolines and related heterocycles. *Green Chem.* **2020**, *22*, 197–203. [[CrossRef](#)]
59. Goncharov, N.; Orekhov, A.N.; Voitenko, N.; Ukolov, A.; Jenkins, R.; Avdonin, P. Organosulfur Compounds as Nutraceuticals. In *Nutraceuticals*; Gupta, R.C., Ed.; Academic Press: Boston, MA, USA, 2016; pp. 555–568. [[CrossRef](#)]
60. Huang, X.; Maulide, N. Sulfoxide-Mediated α -Arylation of Carbonyl Compounds. *J. Am. Chem. Soc.* **2011**, *133*, 8510–8513. [[CrossRef](#)]
61. Carreno, M.C. Applications of Sulfoxides to Asymmetric Synthesis of Biologically Active Compounds. *Chem. Rev.* **1995**, *95*, 1717–1760. [[CrossRef](#)]
62. Shi, J.-L.; Lang, X. Assembling polydopamine on TiO₂ for visible light photocatalytic selective oxidation of sulfides with aerial O₂. *Chem. Eng. J.* **2020**, *392*, 123632. [[CrossRef](#)]
63. Wang, G.; Hu, W.; Hu, Z.; Zhang, Y.; Yao, W.; Li, L.; Fu, Z.; Huang, W. Carbene-catalyzed aerobic oxidation of isoquinolinium salts: Efficient synthesis of isoquinolinones. *Green Chem.* **2018**, *20*, 3302–3307. [[CrossRef](#)]

Disclaimer/Publisher’s Note: The statements, opinions and data contained in all publications are solely those of the individual author(s) and contributor(s) and not of MDPI and/or the editor(s). MDPI and/or the editor(s) disclaim responsibility for any injury to people or property resulting from any ideas, methods, instructions or products referred to in the content.